

Multiple Dot Size Fluidics for Phase Change Piezoelectric Ink Jets

Ronald F. Burr, David A. Tence and Sharon S. Berger
Color Printing and Imaging Division, Tektronix, Inc. Wilsonville, Oregon

Abstract

Ink jet waveform design is a challenge requiring knowledge of ink jet internal dynamics as well as surface dynamics of the aperture and mensicus. Waveforms generally are designed to excite the main driving frequency of the jet, while reducing energy at undesirable resonance frequencies, in order to reliably produce a single drop size. By exciting higher order modes of surface oscillation, drops of several sizes have been produced. Fundamental analysis, computational fluid dynamics simulations and laboratory experimentation have been used to provide a better understanding and demonstration of the drop size modulation process. Application of multiple drop size modulation includes variable resolution and gray scaling printing.

Introduction

Typical drop-on-demand ink jet printers are designed to provide specific print quality at specific speed with a single drop size. Improved print quality can be obtained by increasing resolution while utilizing a smaller drop size. However, this negatively impacts the print speed. With the option of two drop sizes, the user can chose between higher print quality or higher speed as desired. If the drop size can be modulated during a print, grey scale printing can be achieved thus allowing for greater apparent printing resolution without impacting print speed.

Multiple drop sizes can be obtained by appropriate waveform design. In addition to enhanced print modes, waveform design can remove the requirement for particularly small aperture sizes, thus existing production orifice manufacturing technology may be used for higher resolution drop sizes. Eliminating the need for smaller apertures also reduces the susceptibility to contamination.

Whether multiple drop sizes are implemented as two distinct print quality modes or as gray scale printing, the techniques for designing a waveform are the same. The dot size modulation techniques discussed in the paper have been applied successfully for both multiple resolution as implemented in the Tektronix Phaser®340 printer and in laboratory demonstrations of 4-level gray scale printing. Both theoretical and experimental results are discussed. The Tektronix Phaser® 300 phase change ink jet print head was used as the platform for developing multiple drop sizes and will be discussed for the remainder of this paper.

Jet Design Background

Jet design is a complex and iterative process which attempts to satisfy many constraints. However, most basic individual jet design issues can be addressed, at least qualitatively, in terms of the lumped parameter model, and it will be used for this jet design background discussion. Figure 1 is a cross-section of the Phaser® 300 jet stack. Figure 2 shows a corresponding lumped parameter model.

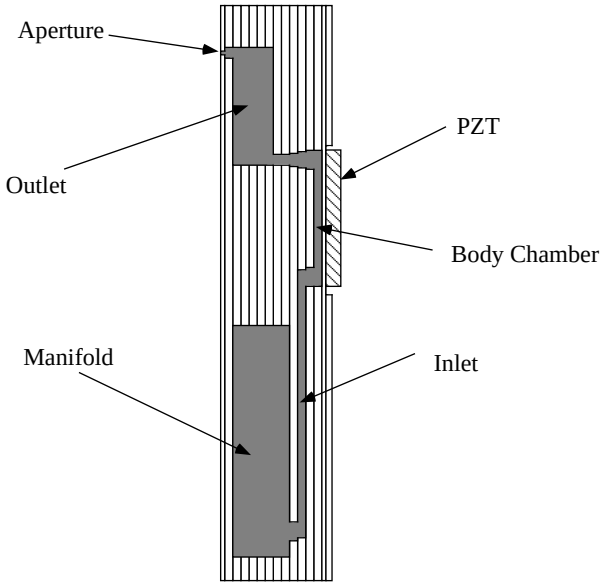

Figure 1. Jet Stack Cross-Section

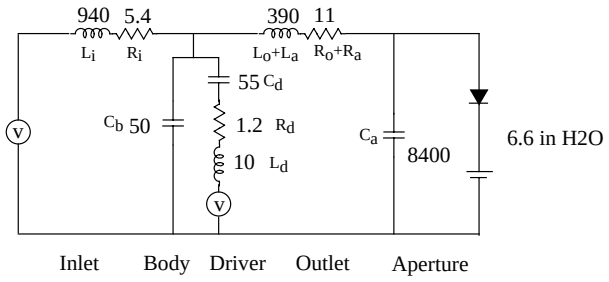

Note: Resistances in mega (M) and capacitance in femto (f).

Figure 2. Lumped Parameter Mode

The basic design requirements are drop size and velocity. For the Phaser 300®, the size and velocity were 200 ng

and 5 m/s, respectively. To estimate the required aperture size, it was assumed that during drop formation the meniscus formed a hemisphere and that after drop formation, half the volume of the aperture was removed (see Figure 3). Based on the drop formation process, described in more detail below, the aperture is generally sized for a volume equal to one drop (200 ng). The aperture diameter for the Phaser® 300 is approximately 75 μm with a length-to-diameter ratio near unity. Once the aperture size has been selected, an inlet size is selected that provides several times larger impedance (Li) than that of the aperture (La) (Figure 2).

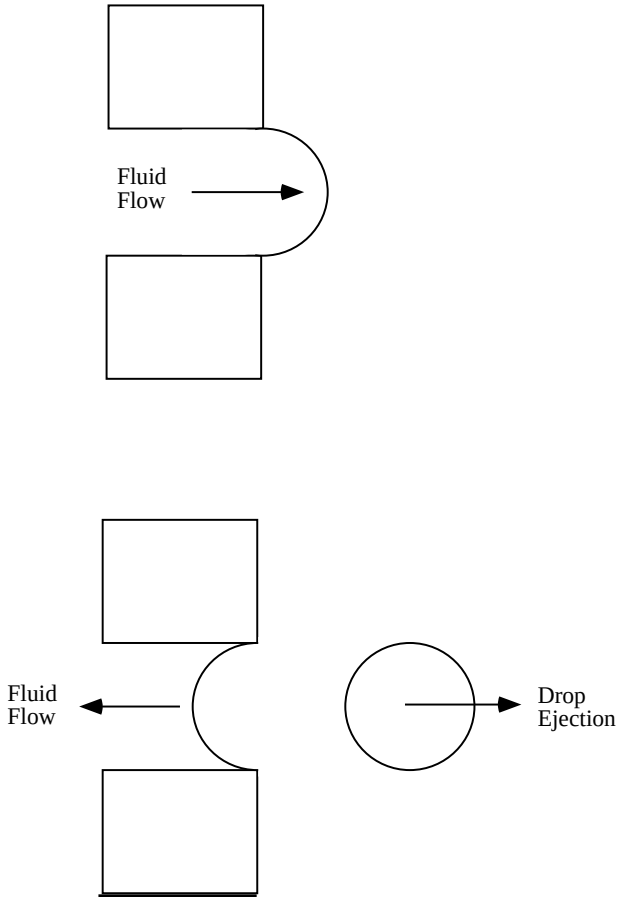

Figure 3. Bulk Mode Drop Ejection

Three fundamental modes are considered in ink jet waveform design: (1) the main or Helmholtz mode (2) the meniscus refill mode and (3) the parasitic standing wave modes. The main mode is directly related to both the drop ejection velocity as well as the maximum repetition rate. It's frequency can be estimated by considering the jet impedance as the inlet inductance (L_i) in parallel with the outlet and aperture inductances (L_o and L_a) and jet capacitance as the combined body fluid (C_b), mechanical (C_d) and outlet (C_o) capacitance (Figure 2).

$$f_m = \frac{1}{2\pi\sqrt{LC}} \qquad (1)$$

$$L = \frac{1}{\frac{1}{L_i} + \frac{1}{L_o + L_a}} \qquad (2)$$

$$C = C_b + C_d + C_o \qquad (3)$$

The Phaser® 300 has an estimated main driving frequency of approximately 25 kHz. Figure 4 is an experimental impedance measurement of an actual jet which confirms the 25 kHz main mode frequency.

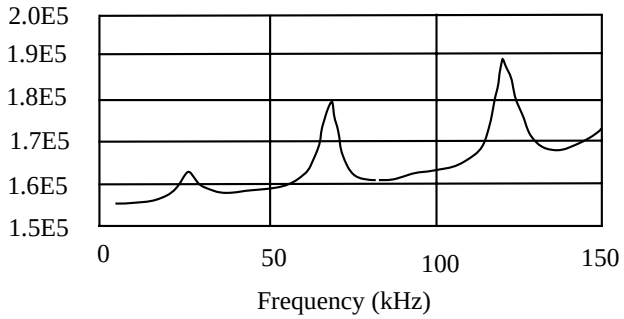

Figure 4. Individual Jet Conductance

A natural frequency of 25 kHz implies that the total length of the waveform must be around 40 μs in order to concentrate energy near the resonance for maximum operating efficiency (Figure 5). Figure 6 is a power spectral density function of the waveform of Figure 5 and shows the energy concentration near, but slightly lower than, the main resonance frequency.

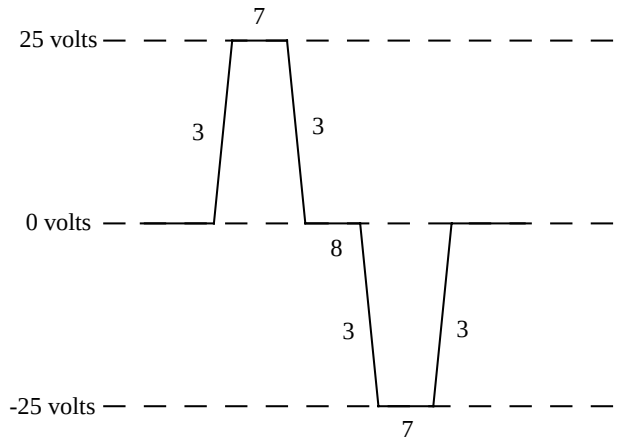

Figure 5. Bulk Mode Drop Waveform

Drop ejection occurs during the high-to-low voltage transition in the center of the waveform of Figure 5. The time of ejection is about one quarter of the total waveform duration (t_e = 10 μs). Drop velocity can be estimated from the drop mass, aperture area, ink density and ejection time and is confirmed to be near the desired value of 5 m/s.

An estimate of the natural meniscus refill time (the time required to refill the aperture after drop ejection) can

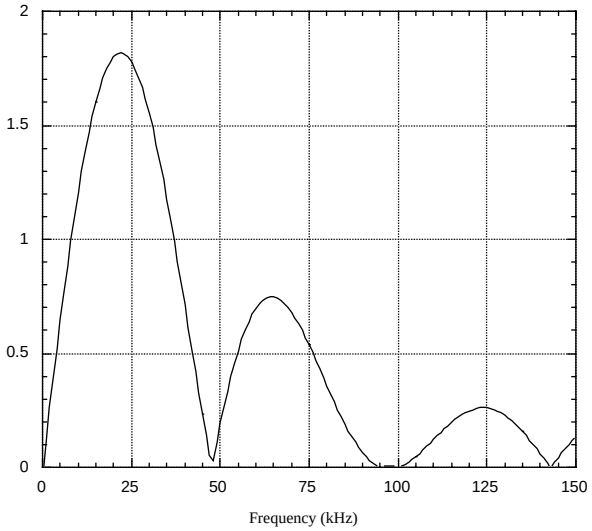

Figure 6. Bulk Mode Waveform Energy Spectrum

be made using the combined resistance of the jet inlet, outlet and aperture and the meniscus capacitance. The mensicus capacitance is estimated based on a the pressure and volume of an hemispherical mensicus after drop ejection (Figure 3). The refill time was estimated to be on the order of 150 μs.

$$\tau_{refill} = (R_i + R_o + R_a)\, C_m \qquad (4)$$

As the natural meniscus refill time is slow compared to the speed of drop formation, the driving waveform is used to enhance the process. The first rising transition in Figure 5 is used to prefill the jet and the final rising transition is used to aid the natural refill process.

Reduction of energy near unwanted resonant mode frequencies is as important as the concentration of energy near the main jet mode frequency for robust, efficient jet performance. Several of these resonances are seen in the experimental impedance measurement of Figure 4. In this figure, the main Helmholtz frequency is at 25 kHz and the unwanted parasitic standing waves are above 30 kHz. Figure 7 shows the corresponding a transmission line model (e.g., Kinsler et al., 1982):[2]

$$Z_0(\omega) + \frac{Z_L(\omega) + j\rho aA\tan(\omega(L/c))}{\rho aA + Z_L(\omega)\tan(\omega(L/c))} \qquad (5)$$

where Z_o is the inlet impedance of the segment under consideration, Z_L is the termination impedance of the segment, which is of cross-sectional area A and length L. The model is used to associate these modes with the inlet and outlet channel standing acoustic waves.

Ideally, these channels would be made very short so that any standing wave frequencies would be much greater than the normal operating frequencies of the jet. This is often not practical when packaging many jets of different color ink into a single print head. Consequently, it is important to choose waveform shapes which minimize the spectral energy near these modes, while still properly exciting the main mode and the desired aperture and mensicus surface wave modes discussed below.

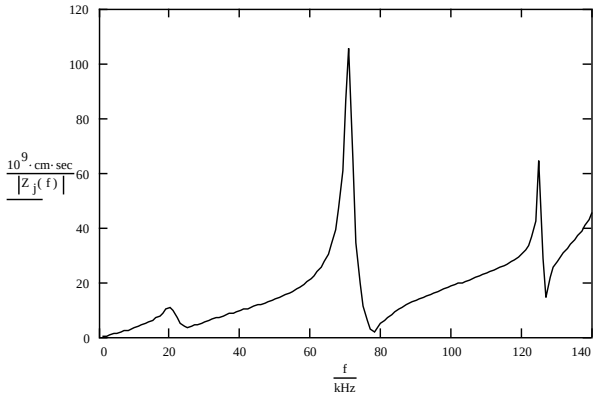

Figure 7. Individual Jet Transmission Line Model

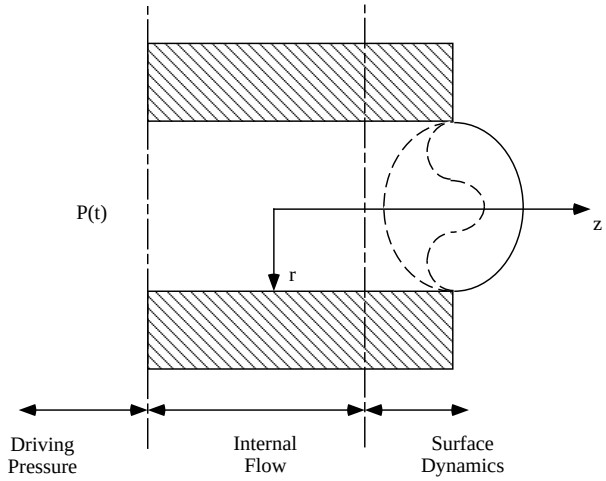

Figure 8. Simplified Aperature Geometry Schematic

Drop Size Modulation Theory

Vibration analysis of a circular membrane provides motivation to attempt to create a higher order mode in the ink jet aperture in order to produce smaller drops. In the analysis, several radial modes of vibration can be excited. These modes can be described with Bessel functions of the first kind. If a meniscus could be excited in a similar way such that flow was moving forward in a reduced portion of the orifice, smaller drop masses could be obtained.

The flow pattern in the aperture is governed by a combination of internal flow (inertial and viscous effects) and meniscus surface dynamics. The orifices considered in the following theoretical description are assumed to be cylindrical. The following analysis of the flow has been separated into three regions as shown in Figure 8. We will describe each region in the following order: (1) surface dynamics, (2) internal flow and (3) driving pressure profile.

Surface Dynamics

To better understand the basic surface dynamics, a potential flow analysis of the orifice flow was performed

(Burr et.al, 1996).[1] The governing fluid dynamic equations and boundary conditions are shown below.

Governing equation:

$$\frac{1}{r}\frac{\partial}{\partial r}\left(r\frac{\partial \phi}{\partial r}\right)+\frac{\partial^2 \phi}{\partial z^2}=0 \tag{6}$$

Boundary conditions:

$$v|_{r=0}=\frac{\partial f}{\partial r}\,|_{r=0}=0 \tag{7}$$

$$v|_{r=R}=\frac{\partial f}{\partial r}\,|_{r=R}=0 \tag{8}$$

$$\phi|_{z=0}=0 \tag{9}$$

$$\left(\frac{\partial^2 f}{\partial t^2}+\frac{s}{r}\left(\frac{1}{r}\frac{\partial}{\partial r}\left(r\frac{\partial}{\partial r}\frac{\partial f}{\partial z}\right)\right)\right)_{z=h}=0 \tag{10}$$

The boundary conditions are applied at the aperture centerline (r = 0), wall at radius R, base of the aperture (z = 0) and free surface at z = h.

A solution is obtained by taking a Laplace transform in time and by separation of variables in the two space dimensions (z and r). The solution in the radial direction takes the form of a Bessel function of the first kind while the axial direction takes the form of hyperbolic functions. Time dependence is assumed to be trigonometric.

$$\phi(r,z,t)=(B_1 \sinh(k_n z)+B_2 \cosh(k_n z))J_0(k_n r)e^{j\omega t} \tag{11}$$

Applying radial boundary conditions and the boundary condition at the aperture base determines the radial mode shapes and the form of the axial variation.

$$\phi(r,z,t)\approx \sinh(\frac{\alpha_n z}{R})J_0(\frac{\alpha_n z}{R})e^{j\omega_n t} \tag{12}$$

Applying the free surface boundary condition determines allowable frequencies of oscillation (modes):

$$\omega_n=\sqrt{\frac{\sigma \alpha_n{}^3}{\rho R^3}\coth\left(\frac{\alpha_n h}{R}\right)} \tag{13}$$

For aspect ratios (h/R) greater than approximately one quarter, the frequency (ω_n) is dependent only on the fluid properties and the aperture diameter:

$$\omega_n\approx\sqrt{\frac{\sigma \alpha_n{}^3}{\rho R^3}} \tag{14}$$

The hyperbolic function confines the surface wave effects to the surface region. The radial mode shape corresponding to the first, second and third modes are shown in Figure 9. For the Phaser® 300 geometry, the first three surface mode frequencies are 35, 55 and 120 kHz, respectively.

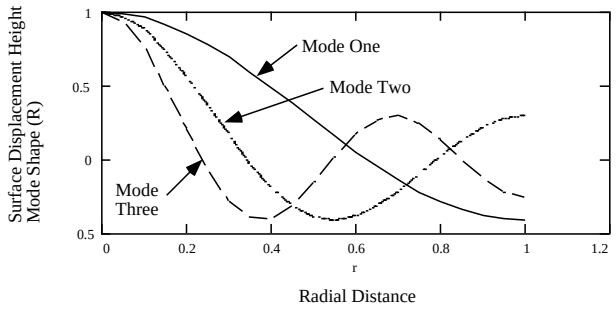

Figure 9. Surface Wave Mode Shapes

Internal Flow Dynamics

To determine whether the viscosity effects were important on the time scale of drop formation, the viscosity effect was estimated for oscillating flow in a pipe with dimensionless time.[3]

$$\tau^*=\frac{\mu \tau}{\rho a^2} \tag{15}$$

For time scales from waveforms which concentrate energy near the 25 kHz main mode frequency and phase change ink properties, this ratio was found to be approximately unity. Thus, the viscous boundary layer effects are significant with the boundary layer profile becoming reasonably fully developed during each cycle of the drop formation process.

A simple model of the inertial-viscous effect was created by considering axially fully-developed flow in a circular duct due to an oscillating pressure gradient:

$$\frac{\partial u}{\partial t}-\frac{\nu}{r}\frac{\partial}{\partial r}\left(r\frac{\partial u}{\partial r}\right)=-\frac{1}{\rho}\frac{\partial p}{\partial x} \tag{16}$$

$$-\frac{1}{\rho}\frac{\partial p}{\partial x}=e^{jwt} \tag{17}$$

$$u(r,t)=R(r)\bullet e^{j\omega t} \tag{18}$$

$$j\omega R-\frac{\nu}{r}\frac{\partial}{\partial r}\left(r\frac{\partial R}{\partial r}\right)=1 \tag{19}$$

Using the above governing equations in the frequency domain, with appropriate no slip boundary conditions at the outer wall, the velocity profile at any input frequency is predicted.

Figures 10 and 11 show the resulting profiles for low and high frequency cases respectively. At lower frequencies (Figure 10) the viscosity causes a parabolic profile which negatively impacts the ability to excite high order surface wave modes. However, at the higher frequencies (Figure 11) viscous effects flatten the velocity profile in the center of the aperture, allowing for surface tension effects to provide surface waves. In fact, the viscous effects cause a slight velocity profile overshoot near the wall at high fre-

quencies which can aid in generating higher order surface modes.

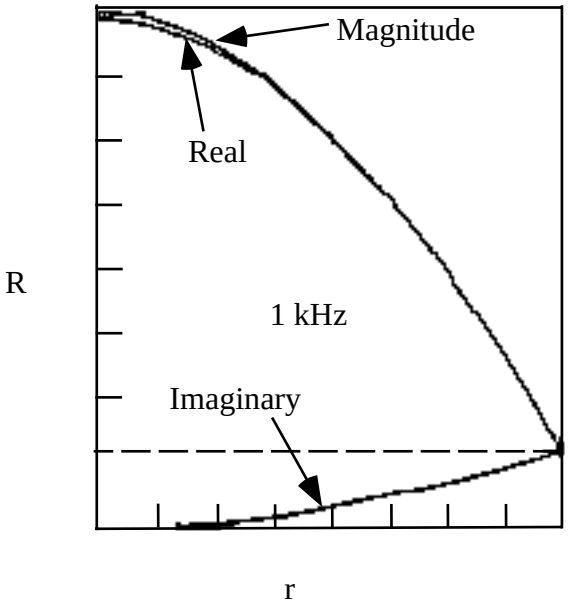

Figure 10. Low Frequency Inertial Viscous Mode

Driving Pressure Profile and Experimental Validation

Once the frequency input required to excite higher order modes is known, the pressure input must be applied behind the jet aperture. However, the dynamics of the jets can dramatically change the input pressure profile shape from that of the input voltage profile. Therefore, before proceeding to the design and demonstration of actual ink jet operation, the fundamental meniscus mode phenomena was demonstrated experimentally using a simple periodic sine wave voltage profile. Sine wave pressure profiles of varying frequency were applied to the jet piezoelectric driver. Figure 12 shows a typical surface wave photograph with a frequency input of approximately 25 kHz. The desired higher order mode shape is clearly evident.

Due to the dynamic complexity of the ink jet itself, it was not possible to quantitatively separate the response due to amplification by the jet resonances from those of the surface resonances. In particular, the maximum surface displacement occurred near the main (Helmholtz) mode resonance frequency of 25 kHz because of the large underdamped amplification factor between the input voltage and the outlet chamber pressure which drives the aperture and meniscus surface flow. In actual ink jet operation, the surface mode excitation must be carefully implemented along with other ink jet and waveform design requirements to provide the desired ink jet performance characteristics.

Application and Results

The above design algorithm was demonstrated by creating a gray scale print from a Phaser® 300 print head and printer. For this demonstration, the existing jet stack geometry was assumed to be fixed. Thus, the only design variable was the driving waveform. To illustrate the ink jet design method,

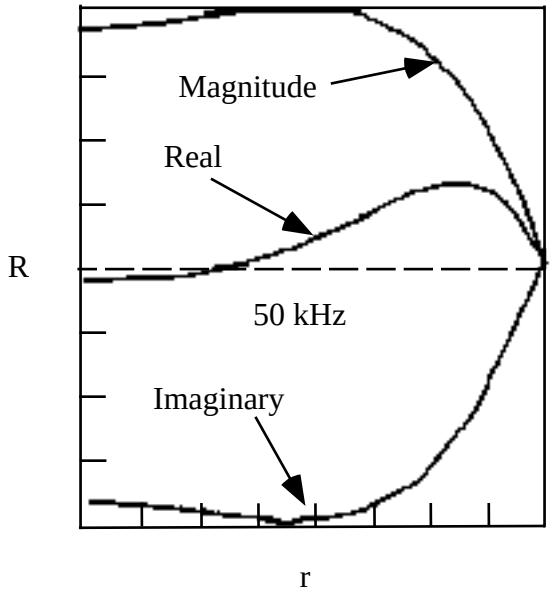

Figure 11. High Frequency Inertial Viscous Mode

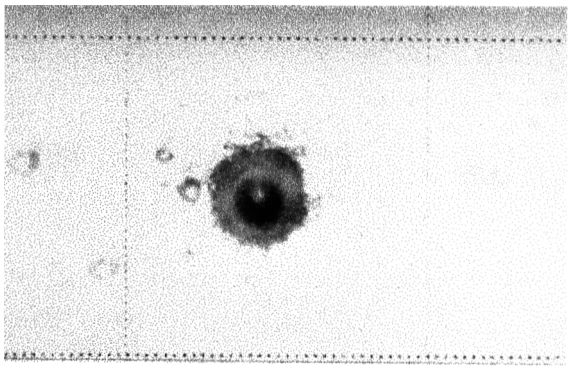

Figure 12. Experimental Meniscus Surface Excitation

only the smallest and most difficult drop size will be considered here. Extension to include a drop size between this small drop and the original large drop was straight forward.

The lower order mode, in which ink jets normally operate, corresponds to a bulk displacement of the orifice fluid forward. Because of surface tension and viscous boundary layer effects, the drop will have the characteristic rounded shape and higher order surface modes will not be present. The natural frequency of this mode is largely determined by the interaction of the bulk motion of a fluid mass with the compression of the fluid internal to the jet (*i.e.*, the main or Helmholtz mode previously discussed). Baseline (standard mode) ink jet design and drive waveform design is based on this mode of operation.

Selection of waveforms to modulate drop size requires additional insight into the natural frequencies of the orifice/meniscus system beyond knowledge of the internal modes of oscillaiton. Analagous to the lower order mode, a waveform is designed to concentrate energy near the natural frequency of the surface mode desired and remove energy from the natural frequencies of competing modes. Following these design guidelines results in efficient and stable jet

operation. Energy near a harmonic of the main mode provides for efficient jet operatrion in terms of being able to excite the desired mode without excessive voltage input. Reducing enery in competing modes, such as interal standing waves or non-axisymmetric menisucs surface modes reduces non-robust performance and off-axis drop flight.

Following the above guidelines, a waveform was designed which maintained the prefill-eject-refill cycle of jet operation, yet concentrated the energy near the higher order surface mode (i.e. 55 kHz). The selected waveform is shown in Figure 13. The corresponding power design spectrum is shown in Figure 14. Energy is concentrated near 55 kHz as well as at low frequencies below the main mode (i.e., below 20-25 kHz). This low frequency energy aids the meniscus refill mode. Energy has clearly been avoided in the main mode band where it would be amplified by the underdamped main resonance mode.

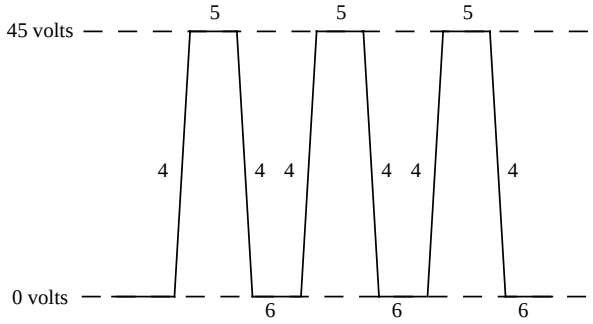

Figure 13. Second Mode Waveform

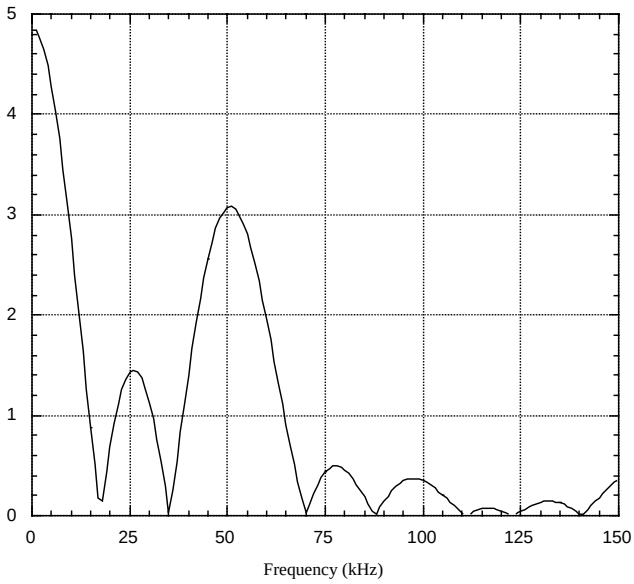

Figure 14. Second Mode Waveform Energy Spectrum

FLOW3D computational fluid dynamics (CFD) software has been instrumental in providing better insight into the design of variable dot size waveforms by modeling the compl.x non-linear flow in the aperture and drop formation. The electronic waveform designed above was applied to the piezoelectric driver in a lumped parameter model of the jet. A simplified version of the aperture pressure profile obtained from the lumped parameter analysis (shown in Figure 15) was used as input to the FLOW3D simulation.

The FLOW3D simulation used an axisymmetric model of the aperture and a portion of the outlet channel just upstream of the aperture along with a free surface for the meniscus and drop formation. The results are shown in Figure 16 from two time steps jet prior to drop release. A small higher order drop of significantly smaller diameter than the aperture is clearly evident. Drop velocities (as indicated by the velocity vectors) were also found to be consistent with the desired velocity (same as the large basic drop to provide convergence at the media surface).

The final step of demonstration is to apply the waveform to the jet in the laboratory. The resulting drop formation was recorded using a strobe and microscope test stand. Figure 17 shows the resulting drop at two delay times approximately corresponding to the drop emergence process shown for the FLOW3D simulation. Figure 17 clearly shows a drop of significantly smaller than the aperture diameter has been created. After adjusting the drive voltage to provide the same flight time as the baseline drop, drop mass was measured at 35 ng, approximately one quarter the baseline.

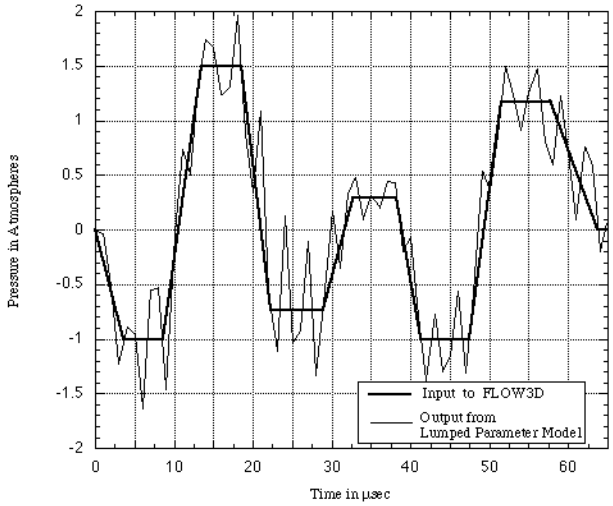

Figure 15. Lumped Parameter Output and Flow 3D Simulation Input

Once the jetting performance had been demonstrated for all three drop sizes, the printhead was used to create 4-level gray scale image quality prints using a modified phase change printer. Image improvements due to the gray scale capability were readily apparent. Another direct application of the modulation capability is to provide selectable resolution modes in a single printer (e.g., without changing aperture size).

Conclusions

A method for creating multiple dot size modulation from piezoelectric ink jet has been presented. Several theoretical models based on simplified linear potential flow and

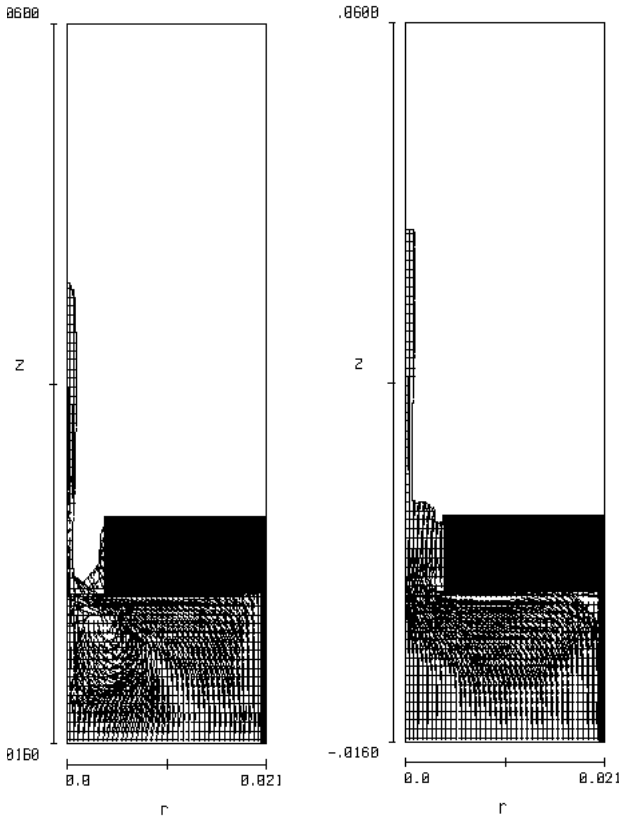

Figure 16. Flow 3D Simulation

laminar duct flow provided insight and design guidance, when combined with existing design procedures (e.g., lumped parameter models). Computational fluid dynamics simulation and laboratory experimentation have provided visualization and validation of the technique for practical multiple mode and gray scale printing devices. However, at the present time a consolidated design or analysis tool does not exist. Such an analysis tool would enhance the ability to understands exploit this phenomena to provide improved ink jet printhead designs.

Acknowledgments

This paper summarizes some of the fluid design aspects of the Phaser® 300 and 340 prototype phase change printheads, which were joint efforts of many employees at the Color Printing and Imaging Division of Tektronix, Inc.

References

1. R. F. Burr, D. A. Tence, H. P. Le, R. L. Adams and J. C. Mutton, "Method and Apparatus for Producing Dot Size Modulated Ink Jet Printing", U.S. Patent 5,495,270, 1996.
2. L. E. Kinsler, , A. R. Frey, A. B. Coppens and James V. Sanders, *Fundamentals of Acoustics*, Third Edition, John Wiley & Sons, New York, 1982.
3. F. M. White, *Viscous Fluid Flow*, McGraw-Hill, New York, 1974.

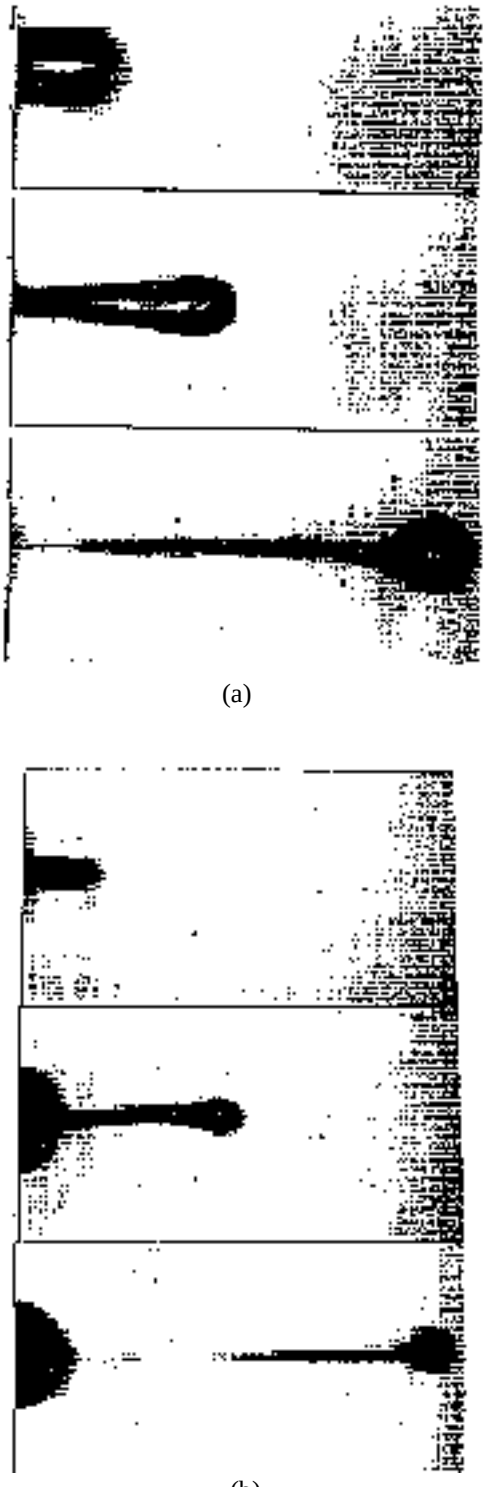

(a)

(b)

Figure 17. Drop Ejection